U.S. DEPARTMENT OF ENERGY

PNNL-22364

Prepared for the U.S. Department of Energy
under Contract DE-AC05-76RL01830

2012 Annual Report: Simulate and Evaluate the Cesium Transport and Accumulation in Fukushima-Area Rivers by the TODAM Code

Y Onishi
ST Yokuda

March 2013

Pacific Northwest
NATIONAL LABORATORY

Proudly Operated by Battelle *Since 1965*

PACIFIC NORTHWEST NATIONAL LABORATORY
operated by
BATTELLE
for the
UNITED STATES DEPARTMENT OF ENERGY
under Contract DE-AC05-76RL01830

Printed in the United States of America

Available to DOE and DOE contractors from the
Office of Scientific and Technical Information,
P.O. Box 62, Oak Ridge, TN 37831-0062;
ph: (865) 576-8401
fax: (865) 576-5728
email: reports@adonis.osti.gov

Available to the public from the National Technical Information Service
5301 Shawnee Rd., Alexandria, VA 22312
ph: (800) 553-NTIS (6847)
email: orders@ntis.gov <http://www.ntis.gov/about/form.aspx>
Online ordering: http://www.ntis.gov


This document was printed on recycled paper.
(8/2010)

PNNL-22364

2012 Annual Report: Simulate and Evaluate the Cesium Transport and Accumulation in Fukushima-Area Rivers by the TODAM Code

Y Onishi
ST Yokuda

March 2013

Prepared for
the U.S. Department of Energy
under Contract DE-AC05-76RL01830

Pacific Northwest National Laboratory
Richland, Washington 99352

Executive Summary

The March 11, 2011, the East Japan Great Earthquake induced a nuclear accident at the Fukushima Daiichi Nuclear Power Plant. This nuclear accident released ^{134}Cs and ^{137}Cs to the environment. Because of the long half-lives of ^{134}Cs and ^{137}Cs, any potential future adverse effects on the environment and human health would be caused by cesium.

Some portions of the ^{134}Cs and ^{137}Cs deposited on land surface were adsorbed by the surface soil and will be washed off from the ground surface to receiving rivers by runoff water and snowmelt. Then, it is expected that the rivers will transport ^{134}Cs and ^{137}Cs downstream to the Pacific Ocean, during which some will be deposited on the river bottom. To conduct the environmental remediation, it is important to evaluate the amounts and locations of cesium accumulation in rivers and radionuclide discharges of dissolved and sediment-sorbed cesium flowing into the Pacific Ocean.

Pacific Northwest National Laboratory initiated the application of the time-varying, one-dimensional sediment-contaminant transport code, TODAM (Time-dependent, One-dimensional, Degradation And Migration) (Onishi et al. 2007) to simulate the cesium migration and accumulation in the Ukedo River in Fukushima. This report describes the preliminary TODAM simulation results of the Ukedo River model from the location below the Ougaki Dam to the river mouth at the Pacific Ocean. The major findings of the 100-hour TODAM simulation of the preliminary Ukedo River modeling are summarized as follows:

- While both the processes of sediment suspension and deposition occurred in the flow, the erosion process dominated in the region from the upstream boundary to a point 16 km from the river mouth.

- The largest deposition occurred in the region between 15 and 16 km from the river mouth.

- Sand was eroded from the bed more than silt and clay were, and silt was eroded from the bed more than clay was.

- The suspension of sand significantly decreased in the region where the largest deposition occurred, while the suspension of both silt and clay continued to increase in the downstream flow direction.

- The dissolved cesium concentration of 1000 Bq/m^3 introduced at the upstream boundary was continuously transported and dispersed, and the cesium adsorption rate of the suspended silt and clay continued to increase in the downstream flow direction.

- In the flow, some of the dissolved cesium was adsorbed by the suspended sand, silt, and clay. Some of the suspended sand, silt, and clay that adsorbed cesium were deposited on the river bottom and some of the cesium was deposited on the bed by adsorption directly from the dissolved cesium in the flow.

- The quantity of cesium adsorbed by the suspended clay was greatest and the suspended sand adsorbed the smallest quantity of cesium.

- The most cesium in the bed layer was deposited through the sediment deposition process except the region between 1 and 2 km from the river mouth.

The preliminary Ukedo River modeling conducted here provides a basis for the detailed analysis of TODAM Ukedo River modeling that will follow.

Acknowledgments

We appreciate the Japan Atomic Energy Agency for having provided us the necessary TODAM simulation input data, e.g., geometry and boundary condition data, of the Ukedo River in Fukushima Prefecture, Japan.

Acronyms and Abbreviations

JAEA	Japan Atomic Energy Agency
PNNL	Pacific Northwest National Laboratory
TODAM	Time-dependent, One-dimensional, Degradation And Migration

Nomenclature

The list shows only the base symbol, without superscripts, subscripts, and the like. The convention used in this document is to modify the base symbol in one or more of the following ways:

- A *j* subscript indicates the value applies to a single sediment fraction, for example, C_j would be the concentration of the j^{th} sediment fraction.
- An *i* subscript indicates the value applies to a single node, for example q_i is the flux past the i^{th} node.
- An (*e*) superscript indicates the value applies to a single segment, or element, and varies with the element's basis function, for example $A^{(e)}(x)$ is a function that describes how the channel's cross-sectional area varies along segment *e*.
- The subscripts 1 or 2 are used with the (*e*) superscript to denote, respectively, the upstream or downstream end of the segment, for example, $A_1^{(e)}$ would represent the channel cross-sectional area at the upstream node of segment *e*.

A	channel cross-sectional area, square meters
B	channel bed width, meters
C_j	j^{th} sediment concentration, or general constituent concentration, kilograms per cubic meter
D	flow depth, meters
d	sediment particle diameter, meters
d_{50}	median diameter of bed sediment, meters
G_j	j^{th} sediment-associated contaminant concentration, Becquerels (Bq) per cubic meter
G_{Bj}	contaminant concentration in j^{th} bed sediments, Becquerels (Bq) or Curies per kilogram
G_w	dissolved contaminant concentration, Becquerels (Bq) per cubic meter
k	the Von Karman value = 0.4
K_j	mass transfer rate between j^{th} suspended sediment-associated and dissolved contaminant, seconds^{-1}
k_a	Nikuradse sand roughness, meters
K_a	armoring coefficient, nondimensional, ranging from 0.0 to 1.0
K_{bj}	mass transfer rate between j^{th} bed sediment associated and dissolved contaminant, seconds^{-1}
K_d	contaminant distribution coefficient, cubic meters per kilogram
L	segment length, meters
M	erodibility coefficient, kilograms per square meter per second
q	constituent flux, kilograms or Bq per day
Q	flow rate, cubic meters per second, cubic meter per day
Q_l	tributary and lateral inflow of water, cubic meters per day per meter or cubic meters per second per meter

Q_{pj} tributary and lateral inflow contribution of j^{th} sediment-associated contaminant, Bq per day per meter or Bq per second per meter

Q_{sj} tributary and lateral inflow contribution of j^{th} sediment, kilograms per day per meter or kilograms per second per meter

Q_T noncohesive sediment transport capacity, kilograms per meter per day

Q_{Ta} actual noncohesive sediment transport rate, kilograms per meter per day

Q_w tributary and lateral inflow contribution of dissolved contaminant, Bq per second per meter

R channel hydraulic radius, meters

S channel slope, nondimensional

S_{Dj} j^{th} sediment deposition rate, kilograms per square meter per day

S_{Rj} j^{th} sediment erosion rate, kilograms per square meter per day

t time, days or seconds

U longitudinal flow velocity, meters per day or meters per second

U_* shear velocity, meters per day or meters per second

x station or longitudinal coordinate, meters

γ specific weight of sediment solids, kilograms (force) per cubic meter

γ_w specific weight of water, kilograms (force) per cubic meter

Δt simulation time step, days

ε_x longitudinal dispersion coefficient, square meters per second

λ radioactive decay rate, $days^{-1}$ or $seconds^{-1}$

ρ water density, kg per cubic meter

v_s effective particle settling velocity, meters per day or meters per second

τ_b bed shear stress, kilograms per square meter

τ_{R_c} critical shear stress for erosion, kilograms per square meter

τ_{D_c} critical shear stress for deposition, kilograms per square meter

Φ basis function

Contents

Figures

Tables

1.0 Introduction

The March 11, 2011, East Japan Great Earthquake induced a nuclear accident at Fukushima Daiichi Nuclear Power Plant. This nuclear accident released ^{131}I, ^{134}Cs and ^{137}Cs to the environment, in addition to very small amounts of ^{89}Sr, ^{90}Sr, ^{238}Pu, and $^{239-240}Pu$. Because the half-lives of ^{134}Cs and ^{137}Cs (2.06 and 30.0 years, respectively) are long compared to ^{131}I (8.04 days), any potential future adverse effects on the environment and human health would come from cesium. Airborne cesium deposited on the land surface binds tightly to soil, especially clay and fine silt, and cesium has not migrated much down into the subsurface environment. Figure 1.1 shows a ^{137}Cs distribution on the land surface and direct radiation exposure from ^{134}Cs and ^{137}Cs on the land surface (MEXT 2011).

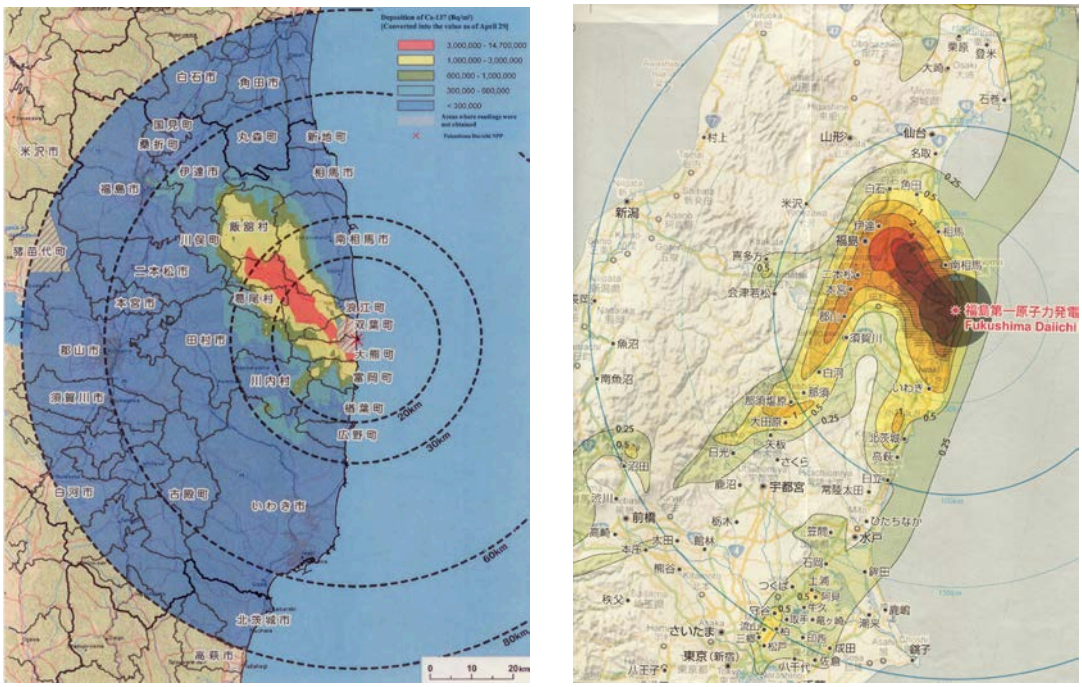

Figure 1.1. Measured ^{137}Cs Distribution on the Land Surface and Measured Direct Radiation Exposure from the Land Surface (MEXT 2011)

Some portions of the ^{134}Cs and ^{137}Cs released from the Fukushima Daiichi Nuclear Power Plant in 2011 and adsorbed by the surface soil will be washed off from the ground surface to receiving rivers by runoff water and snowmelt. To conduct environmental remediation, it is important to evaluate the amounts and locations of cesium accumulation in rivers and radionuclide discharges of dissolved and sediment-sorbed cesium flowing into the Pacific Ocean. Cesium released from the Fukushima Daiichi Nuclear Power Plant is tightly bound to soil. Assessing the cesium behavior in the Fukushima-area rivers is important in light of the current situation that remediation of contaminated forests is difficult.

Rivers move cesium downstream, deposit particulate cesium on the river bottom, and resuspend particulate cesium from the river bottom. Meanwhile cesium undergoes adsorption to and desorption from sediment, as well as radionuclide decay. As river water moves toward the ocean, cesium adsorption

to sediment decreases, desorption from sediment increases, and consequently the dissolved cesium concentration increases, due to changes from fresh water to salty water.

Pacific Northwest National Laboratory (PNNL) has been providing technical assistance to the Japan Atomic Energy Agency's (JAEA's) effort to analyze, test, and evaluate issues associated with the recovery and stabilization of areas contaminated by the 2011 Fukushima Nuclear Plant accident. Currently, PNNL is assisting environmental remediation activities, as well as evaluating the cesium migration from the land surface to rivers and in-stream migration and accumulation of cesium eroded from the land surface. PNNL initiated the application of the PNNL-developed one-dimensional code TODAM (Time-dependent, One-dimensional, Degradation And Migration) (Onishi et al. 2007) to determine the cesium migration and accumulation in Fukushima-area rivers. Simulation results will identify critical locations, and will estimate the cesium accumulation and its future changes in the rivers and the amount and timing of cesium discharged into the Pacific Ocean.

This report describes preliminary TODAM simulation results of the Ukedo River in Fukushima from the Ougaki Dam to the river mouth at the Pacific Ocean, as shown in Figure 1.2. In this figure, north is upward, and the Fukushima Daiichi Nuclear Power Plant located on the coast of the Pacific Ocean is indicated by the red dot. Blue boxes show five local rivers (the Otaka, the Ukedo, the Maeda, the Kuma, and the Tomioka rivers) draining to the Pacific Ocean. An additional five inland rivers shown in this figure are tributaries of these coastal rivers. Orange boxes in this figure show the names of five dams in these rivers. The Ukedo River is the second river north of the Fukushima Daiichi Nuclear Plant, and the Ougaki Dam is 22 km from the Ukedo river mouth. In Figure 1.3, the horizontal axis the distance in km from the river mouth at the Pacific Ocean. The vertical axis indicates the Ukedo River's elevations (green, right axis) and widths (blue, left axis).

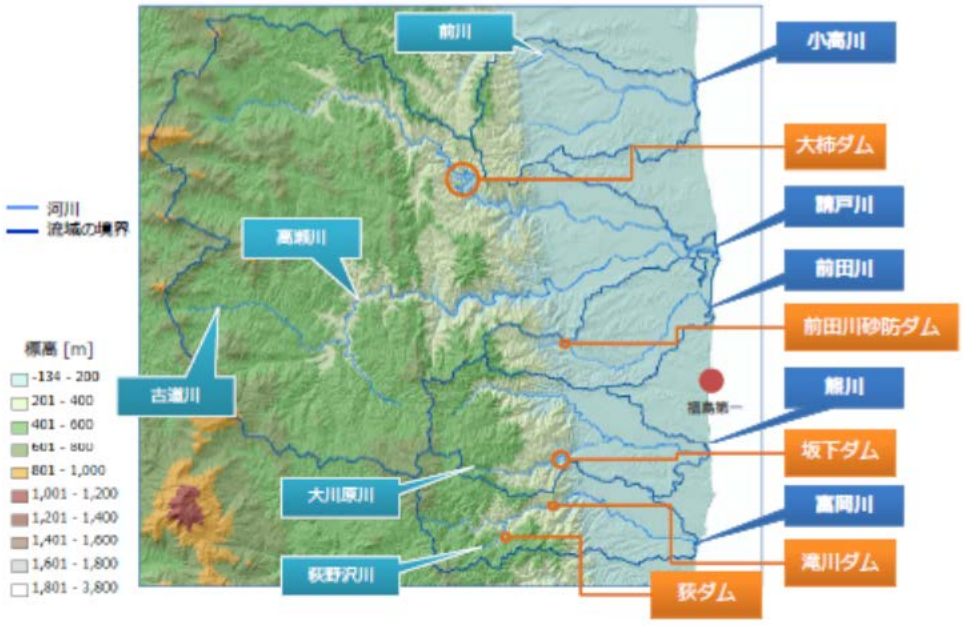

Figure 1.2. The Ukedo River and other Nearby Rivers in Fukushima Prefecture, Japan

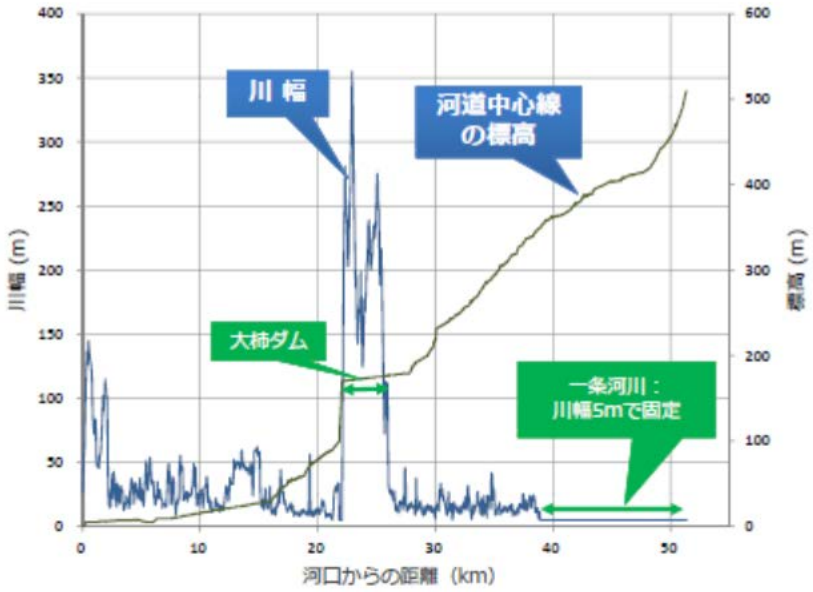

Figure 1.3. The Ukedo River's Elevation and Width Changes

TODAM simulation results will be evaluated to identify critical locations, timing, the amount of cesium accumulation in the rivers and its expected future change, and the amount and timing of cesium discharged into the Pacific Ocean. These evaluation results will assist ongoing and future environmental remediation activities and policies in a systematic and comprehensive manner. For example, the evaluation would help address the following aspects:

- Is the current environmental remediation appropriate?
- What are the beneficial effects of specific remediation activities?
- Where and how much remediation is needed to protect the future public safety?
- Whether recontamination would occur, e.g., whether decontaminated agricultural fields will remain clean in future.
- Whether the river water will be safe for domestic and agricultural usage.
- Whether forests need to be remediated.
- Whether installing settling ponds in rivers would be useful to trap sediment-sorbed cesium. If so, where, and how large, should settling ponds be?
- How much cesium would be transported out into the Pacific Ocean? Will it be a significant amount? Is cesium mostly associated with suspended sediment? What are the expected dissolved cesium concentrations when it reaches ocean beaches?

2.0 TODAM Model Description

TODAM is a finite-element, time-varying, one-dimensional code to simulate sediment and contaminant transport in rivers and estuaries both in water columns and within river-estuarine bottoms (Onishi et al. 2007). It consists of three submodels of sediment, dissolved contaminant, and sediment-sorbed contaminant transport to simulate sediment and contaminant migration along with their interactions, e.g., adsorption-desorption with sediment, transport, deposition and resuspension of sediment and sediment-sorbed contaminants. Sediment is divided into three size fractions, usually one noncohesive sediment (e.g., sand), and the other two for cohesive sediment, (e.g., silt and clay) and/or an organic material.

TODAM was developed by PNNL to predict time-varying longitudinal distributions of the following parameters.

- In the river water column
  - concentrations of
    - suspended sand
    - suspended silt
    - suspended clay
  - dissolved radionuclide concentration
  - particulate radionuclide concentrations adsorbed by
    - suspended sand
    - suspended silt
    - suspended clay
- In the river bed at any given downstream location
  - river bed elevation change caused by sediment erosion and deposition
  - vertical distributions of sediment fractions of
    - bottom sand
    - bottom silt
    - bottom clay
  - vertical distributions of radionuclide concentrations adsorbed by
    - bottom sand
    - bottom silt
    - bottom clay.

It predicts these concentrations by solving the conservation of mass.

2.1 Sediment Transport

Because the movements and contaminant adsorption capacities of sediments vary significantly with sediment sizes, the sediment transport submodel describes the migration of sediment (transport, deposition, and resuspension) for three sediment size fractions of cohesive and noncohesive sediments. The sediment transport submodel includes mechanisms of

1. advection and dispersion of sediments;
2. fall velocity and cohesiveness;
3. deposition on the river and estuarine bed;
4. resuspension from the river and estuarine bed; and
5. sediment contributions from tributaries and point and nonpoint sources into the river and estuarine systems.

Sediment mineralogy and water quality effects are implicitly included through Mechanisms 2, 3, and 4 above.

Mass conservation of sediment passing through a control volume leads to the following expression for the one-dimensional sediment transport with the help of the equation of continuity:

$$A\frac{\partial C_j}{\partial t}+UA\frac{\partial C_j}{\partial x}=\frac{\partial}{\partial x}\left(\varepsilon_x A\frac{\partial C_j}{\partial x}\right)-Q_l C_j+B\left(S_{R_j}-S_{D_j}\right)+Q_{S_j} \tag{2.1}$$

where
C_j = the concentration of sediment of the j^{th} size fraction, kilograms per cubic meter;
A = channel cross-sectional flow area, square meters;
B = channel bed width, meters;
Q_{sj} = sediment contribution of the j^{th} size fraction from tributary and/or lateral inflow, kilograms per meter per day;
S_{Dj} = deposition rate of sediment, kilograms per square meter per day;
S_{Rj} = erosion rate of bed sediment, kilograms per square meter per day;
U = longitudinal flow velocity, meters per day;
ε_x = longitudinal dispersion coefficient, square meters per day; and
Q_l = net lateral inflow, cubic meters per day per meter.

TODAM simulates the transport of three separate sediment size classes using Equation 2.1. These classes are nominally called “sand,” “silt” and “clay” in this document. The “sand” class is considered to be noncohesive; “silt” and “clay” are both considered to be cohesive. Erosion and deposition, represented by S_R and S_D in Equation 2.1, are computed differently for cohesive and noncohesive sediment classes. For noncohesive sediment (“sand”), S_R and S_D are computed as

$$S_R=\begin{cases}K_a\left(\dfrac{Q_T-Q_{T_a}}{\Delta x}\right), \text{ for } Q_T>Q_{T_a}\\ 0.0, \text{ for } Q_T\le Q_{T_a}\end{cases} \tag{2.2}$$

and

$$S_D=\begin{cases}K_a\left(\dfrac{Q_{T_a}-Q_T}{\Delta x}\right), \text{ for } Q_{T_a}>Q_T\\ 0.0, \text{ for } Q_{T_a}\le Q_T\end{cases} \tag{2.3}$$

where K_a = an armoring coefficient, ranging from 0.0 to 1.0;
Q_T = the (noncohesive) sediment transport capacity, kilograms per meter (of width) per day;
Q_{T_a} = the actual sediment transport rate, kilograms per meter per day; and
Δx = the length of the stream segment under consideration, meters.

Erosion rates are limited by available bed sediment (see Section 2.6). Three methods are available in TODAM to compute sediment transport capacity:

- The *Du Boys* method (Du Boys 1879) as described by Vanoni (1975);
- The *Toffaleti* formula (Toffaleti 1969), as described by Vanoni (1975); and
- The *Colby* method (Colby 1964) as described by Vanoni (1975).

Erosion and deposition of cohesive sediment fractions are estimated by formulas of Partheniades (1962) and Krone (1962):

$$S_R = \begin{cases} K_a M\left(\frac{\tau_b}{\tau_{R_c}} - 1\right), \text{ for } \tau_b \geq \tau_{R_c} \\ 0.0, \text{ for } \tau_b < \tau_{R_c} \end{cases} \quad (2.4)$$

and

$$S_D = \begin{cases} C v_s\left(1 - \frac{\tau_b}{\tau_{D_c}}\right), \text{ for } \tau_b \leq \tau_{D_c} \\ 0.0, \text{ for } \tau_b > \tau_{D_c} \end{cases} \quad (2.5)$$

where
M = erodibility coefficient, kilograms per square meter per day;
τ_b = the bed shear stress, kilograms per square meter;
τ_{D_c} = the critical bed shear stress for deposition, kilograms per square meter;
τ_{R_c} = the critical bed shear stress for erosion, kilograms per square meter; and
v_s = the effective particle settling velocity, meters per day.

In TODAM, bed shear stress, τ_b, can be read as input data, or it can be estimated in one of two ways within TODAM. The first is used for running streams with a nonzero slope:

$$\tau_b = \gamma_w SR \quad (2.6)$$

where τ_b = bed shear stress, kilograms per square meter;
γ_w = the specific weight of water, kilograms (force) per cubic meter;
S = the channel bottom slope, meters per meter; and
R = the channel's hydraulic radius, meters.

The second method is more suited to reservoirs, for example, where the energy slope is different from the channel slope:

$$\tau_b = \frac{\rho}{g} U_*^2 \tag{2.7}$$

where g = the acceleration of gravity, meters per square second; and
U_* = the shear velocity, meters per second

which is computed by Graf (1971), as

$$U_* = \frac{U}{17.66 + \frac{2.3}{k} \log\left(\frac{D}{96.5 k_a}\right)}$$

where D = the flow depth, meters;
k_a = the Nikuradse sand roughness, meters, which
= the median bed sediment diameter, d_{50}, according to Chow (1959); and
K = the Von Karman value = 0.4.

2.2 Sediment-Sorbed Contaminant Transport

The transport submodel of contaminant attached to sediment includes the mechanisms of

1. advection and dispersion of particulate (sediment-sorbed) contaminant;
2. adsorption of dissolved contaminant by both moving (suspended and bed-load sediment) and stationary bottom sediment or desorption from these sediments into water;
3. radioactive decay;
4. deposition of particulate contaminant to the river and estuary bed or resuspension from the bed; and
5. contributions of particulate contaminants from tributaries and point and nonpoint sources into the river and estuarine systems.

As in the sediment transport, conservation of contaminant adsorbed by each size fraction of three sediment sizes may be expressed with the help of the equation of continuity as

$$\begin{aligned} A\frac{\partial G_j}{\partial t} + UA\frac{\partial G_j}{\partial x} &= \frac{\partial}{\partial x}\left(\varepsilon_x A \frac{\partial G_j}{\partial x}\right) - \lambda A G_j - Q_l G_j \\ &+ B\left(G_{B_j} S_{R_j} - \frac{S_{D_j} G_j}{C_j}\right) + Q_{p_j} + A K_j \left(K_{d_j} C_j G_w - G_j\right) \end{aligned} \tag{2.8}$$

where G_j = the concentration of contaminant associated with the j^{th} sediment fraction, Becquerels (Bq) per cubic meter;
λ = the contaminant radioactive decay rate, day^{-1};

G_{B_j} = the contaminant concentration in bed sediments of the j^{th} fraction, Bq per kilogram;

Q_{P_j} = the contribution of contaminant associated with the j^{th} sediment size fraction from tributary and lateral inflow, Bq per meter per day;

K_j = the mass transfer rate for dissolved contaminant adsorption to and desorption from suspended sediment of the j^{th} fraction, day^{-1};

K_{d_j} = the distribution coefficient between dissolved contaminant and sediment-associated contaminant in the j^{th} sediment fraction (both suspended and bed), cubic meters per kilogram; and

G_w = the dissolved contaminant concentration, Bq per cubic meter.

TODAM simulates the transport of contaminant associated with three separate sediment size classes using Equation 2.8.

2.3 Dissolved Contaminant Transport

The dissolved contaminant transport submodel includes the following mechanisms:

1. advection and dispersion of dissolved contaminant;
2. adsorption of dissolved contaminant by each size fraction of moving (suspended and bed-load sediments) and stationary bottom sediment or desorption from these sediments into water;
3. degradation of dissolved contaminant due to hydrolysis, oxidation, photolysis, and microbial activities;
4. volatilization;
5. radioactive decay; and
6. contributions from tributaries and point and nonpoint sources into the river and estuarine systems.

Effects of water quality (for example, pH, water temperature, salinity) and clay minerals on contaminant adsorption and desorption are taken into account through changes in the distribution coefficients for adsorption and desorption, K_{d_j}.

Conservation of dissolved contaminant in a control volume may expressed as

$$\begin{aligned} A\frac{\partial G_w}{\partial t} + UA\frac{\partial G_w}{\partial x} &= \frac{\partial}{\partial x}\left(\varepsilon_x A\frac{\partial G_w}{\partial x}\right) \\ &- \lambda A\, G_w - \sum_{i=1}^{5} K_{C_i} A\, G_w - Q_l G_w + Q_w \\ &- \sum_{j=1}^{N_f} A\, K_j\left(K_{d_j} C_j G_w - G_j\right) \\ &- \sum_{j=1}^{N_f} B\,\gamma_j (1-n) d_j K_{b_j}\left(K_{d_j} G_w - G_{B_j}\right) \end{aligned} \tag{2.9}$$

where K_{C_i} = first-order reaction rates of dissolved contaminant degradation from causes other than radioactive decay, days^{-1};
Q_w = the contribution of dissolved contaminant from tributary and lateral inflow, Bq per meter per day;
γ_j = the solids density of the j^{th} sediment size fraction, kilograms per cubic meter;
n = bed sediment porosity;
d_j = (median) particle diameter of the j^{th} sediment fraction, meters; and
K_{b_j} = mass transfer rate for dissolved contaminant adsorption to and desorption from the j^{th} bed sediment fraction, days^{-1}.

The K_{C_i} rate constants are used in Equation 2.9 to account for volatilization and for chemical and biological degradation due to

1. hydrolysis,
2. oxidation,
3. photolysis,
4. microbial activities.

2.4 Discretization and Solution

TODAM uses the Galerkin finite-element method to estimate solutions to the sediment and contaminant transport equations (Equations 2.1, 2.8 and 2.9) in space. In the Galerkin method, the problem domain is divided into smaller "elements" or "segments." Each segment is considered to have a "node" at each end. A set of equations is computed for each segment in the domain. These have the form

$$[P^{(e)}]\left\{\frac{da}{dt}\right\} + [S^{(e)}]\{a\} = \{R^{(e)}\} \tag{2.10}$$

where vector $\{a\}$ is the approximation of concentration at the ends of the segment. These equations are called the typical or local element equations. Once computed, the local element equations are assembled (by linear combinations) into a system of equations for the entire domain. These have the form

$$[P]\left\{\frac{da}{dt}\right\} + [S]\{a\} = \{R\} \tag{2.11}$$

where the vector $\{a\}$ is the approximation of concentration at all nodes in the domain. In TODAM it is assumed that

$$a = \theta a^t + (1-\theta)\, a^{t+\Delta t}$$

where θ is between 0 and 1. Substituting this into Equation 2.5 produces

$$[P]\frac{\{a\}^{t+\Delta t}-\{a\}^{t}}{\Delta t} = -[S]\left(\theta\{a\}^{t}+(1-\theta)\{a\}^{t+\Delta t}\right)+\{R\}$$

Solving for the future time step, $t + \Delta t$, the above equation becomes

$$[P]\{a\}^{t+\Delta t}=[S]\{a\}^{t}+\{R\} \tag{2.12}$$

where the new coefficient matrices are

$$[P]=[P]+(1-\theta)\,\Delta t\,[S] \tag{2.13}$$

$$[S]=[P]-\theta\Delta t\,[S] \tag{2.14}$$

and

$$\{R\}=\Delta t\,\{R\} \tag{2.15}$$

Certain equations in the system of Equation 2.12 are replaced with boundary conditions and junction mass-balance equations. The system is then solved for the concentrations at each node.

2.5 Channel Branching

Although TODAM is a one-dimensional code, it can handle channel branching with the use of "junctions." A "junction" is a collection of nodes where several rivers merge and/or diverge (Figure 2.1). At a junction, sediment and contaminant mass are balanced by setting the sum of both advective and dispersive fluxes into the junction equal to zero:

$$\sum_{i=1}^{N_j}\left(Q_i C_i-\varepsilon_x A_i\frac{dC}{dx}\bigg|_i\right)=0 \tag{2.16}$$

where N_j = the number of nodes in the junction.

The concentration gradient at a node needs to be estimated. This is done using the concentration at the nearest node. For example, the concentration gradient for node 3 in Figure 2.1 (a) would be estimated as

$$\frac{dC}{dx}\bigg|_3 \approx \frac{C_4-C_3}{L^{(b)}} \tag{2.17}$$

Applying the mass balance to the confluence situation shown in Figure 2.1 results in

$$Q_3C_3 + \varepsilon_x^{(b)}A_3\frac{C_4 - C_3}{L^{(b)}} + Q_5C_5 + \varepsilon_x^{(c)}A_5\frac{C_6 - C_5}{L^{(c)}} - Q_2C_2 - \varepsilon_x^{(a)}A_2\frac{C_2 - C_1}{L^{(a)}} = 0 \quad (2.18)$$

Figure 2.1 (b) results in

$$Q_2C_2 + \varepsilon_x^{(a)}A_2\frac{C_1 - C_2}{L^{(b)}} - Q_5C_5 - \varepsilon_x^{(c)}A_5\frac{C_5 - C_6}{L^{(c)}} - Q_3C_3 - \varepsilon_x^{(b)}A_3\frac{C_3 - C_4}{L^{(b)}} = 0 \quad (2.19)$$

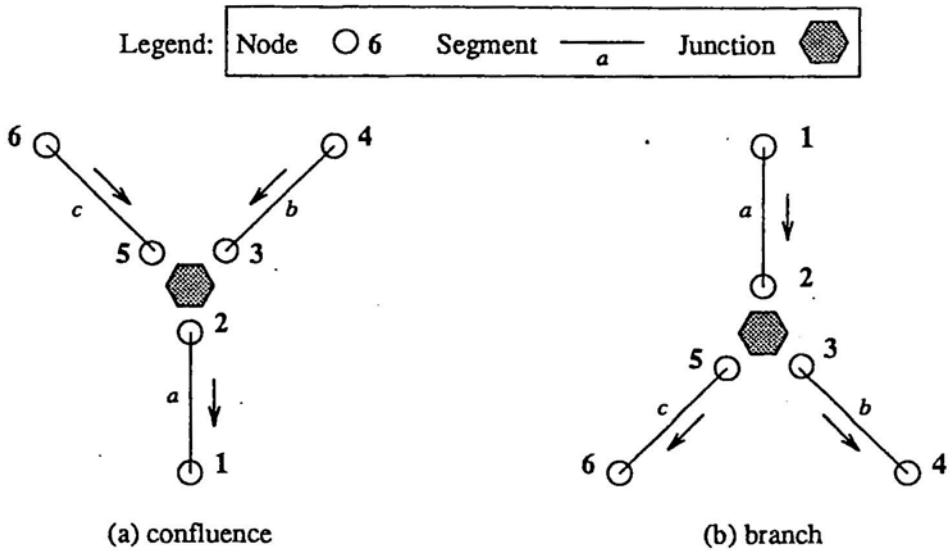

Figure 2.1. Schematics of Two Cases where Junctions are Used. See text for an explanation of how these cases are simulated.

Additionally, the condition that all outflow node concentrations must be equal, in this case $C_3 - C_5 = 0$, is linearly combined with the equation for the remaining outflow nodes (in this case node 5).

2.6 Bed Materials Accounting

TODAM maintains an accounting of available bed materials. These materials are affected by erosion/deposition and adsorption/desorption predicted by the sediment and contaminant transport submodels. Bed materials are conceptualized as a series of horizontal material layers, of some "standard" thickness, *T*, lying above an unerodable bedrock. The standard layer thickness is constant within a

segment but may vary from segment to segment. The materials have a spatially constant (within a segment) porosity which is assumed to be completely filled with water. The accounting performed by TODAM considers the following:

- erosion from and deposition to bed materials;
- contaminant decay within bed materials; and
- contaminant movement (diffusion) within bed materials.

3.0 Ukedo River Modeling

In order to evaluate the amounts and locations of cesium accumulation in rivers and radionuclide discharges of dissolved and sediment-sorbed cesium flowing into the Pacific Ocean, the time-varying, one-dimensional sediment-contaminant transport code TODAM was applied to the Ukedo River in Fukushima from the location below the Ougaki Dam to the river mouth at the Pacific Ocean.

This chapter describes the performed Ukedo River TODAM modeling and presents the preliminary model results.

3.1 Description of the Ukedo River

The variations of the elevation (thalweg) and width of the Ukedo River were provided by the Japan Atomic Energy Agency (JAEA) and are given in Figure 1.3. As seen in Figure 1.3, the Ukedo River includes the Ougaki Dam located at about 22 km from the river mouth at the Pacific Ocean. The river slope in the upstream is very steep until it reaches a location at about 16 km from the river mouth. As the stream passes a location about 6 km from the river mouth, the river slope becomes gentle.

Another characteristic of the Ukedo River is that it merges with the the Takase River at about 2 km from the river mouth (see Figure 1.2). Figure 1.3 shows that this confluence of the Ukedo and the Takase rivers results in the large river width with the maximum above 140 m. In addition, Figure 1.3 shows that the river width widens to about 50 m in the region between about 13 km and about 15 km from the river mouth. Then, the flow velocity in this region decreases.

As a preliminary simulation, the TODAM modeling was conducted for the region from the location below the Ougaki Dam to the river mouth at the Pacific Ocean. JAEA has provided PNNL with the geometry and flow rate data used for the TODAM modeling. Table 3.1 shows the provided geometry and flow rate data.

Table 3.1 shows that the flow rate increases from 4.19 to 6.28 m^3/s in the region from the start point of the modeling, 22 km, to the point 16 km from the river mouth. The lateral inflow of the runoff water into the river is assumed to be responsible for this increase in the flow. In addition, the confluence of the Ukedo and the Takase rivers, as mentioned above, is considered to cause the flow rate increase from 6.28 to 12.56 m^3/s at the point 1 km from the river mouth.

The data of the geometry and flow rate with the flow depth and cross-sectional area used for the TODAM simulation are described in detail in the next section.

Table 3.1. Geometry and Flow Rate of the Ukedo River Provided by JAEA.

Distance from River Mouth (m)	Flow Rate (m3/s)	Elevation (m)	Width (m)
22000	4.19	102.00	10.0
21000	4.54	90.00	10.0
20000	4.88	78.00	10.0
19000	5.23	66.00	10.0
18000	5.58	54.00	10.0
17000	5.93	42.00	20.0
16000	6.28	30.00	20.0
15000	6.28	27.50	50.0
14000	6.28	25.00	50.0
13000	6.28	22.50	50.0
12000	6.28	20.00	20.0
11000	6.28	17.50	20.0
10000	6.28	15.00	20.0
9000	6.28	12.50	20.0
8000	6.28	10.00	20.0
7000	6.28	7.50	20.0
6000	6.28	5.00	20.0
5000	6.28	4.17	20.0
4000	6.28	3.33	20.0
3000	6.28	2.50	20.0
2000	6.28	1.67	80.0
1000	12.56	0.83	80.0
0	12.56	0.00	30.0

3.2 Ukedo River Modeling

As mentioned in the previous section, the TODAM modeling of the Ukedo River was conducted for the region from the location below the Ougaki Dam to the river mouth at the Pacific Ocean on the basis of the geometry and flow rate data given in Table 3.1.

Because the time-varying, one-dimensional sediment-contaminant transport code TODAM does not simulate the hydrodynamics of rivers, the flow data are needed for the TODAM simulation as the input data. In this Ukedo River modeling, the CHARIMA code (Holly et al. 1990) developed by the Iowa Institute of Hydraulic Research was used to evaluate the flow parameters used for the Ukedo River modeling by TODAM with the data provided in Table 3.1.

CHARIMA executes finite-difference approximations to solve the flow-sediment equations with the following hypotheses (Holly et al. 1990):

- The flow is one-dimensional.
- A hydrostatic pressure distribution prevails at any point in the channel.
- The resistance laws for steady-state flow are applicable to unsteady flow.
- The channel bed slope is small.

Since the flow data are supplied to the TODAM simulation as the input data, it is assumed that the flow field is independent of the bed-evolution (bed erosion and sediment accumulation) process in the TODAM modeling; namely, the effect of the bed evolution is assumed to be negligible on the flow field in the TODAM modeling.

Table 3.2 presents the flow parameters evaluated by CHARIMA. The values of the elevation (thalweg) and depth in Table 3.2 are as same as the ones given in Table 3.1, which were provided by JAEA, at each station. However, the flow rates at the stations at 21, 19, and 17 km differ from the ones given in Table 3.1. The different values were used for the TODAM simulation because CHARIMA requires at least two node points to evaluate the flow rate and it was deemed to be unnecessary to increase the node number for the TODAM simulation herein.

For the CHARIMA run, the inflow rate of 4.19 m^3/s was used as the upstream boundary condition. For the downstream boundary condition, the flow depth of 0.63 m was used as this value provides 0.03 of the Manning number from the following equation (see also in Table 3.2):

$$n_M = \frac{1}{U}\left(\frac{A}{B+2D}\right)^{2/3} S^{0.5} \tag{3.1}$$

where n_M = Manning number,
U = flow velocity,
A = flow area,
B = flow width,
D = flow depth, and
S = channel slope.

The flow areas and depths given in Table 3.2 were evaluated by CHARIMA for Manning numbers of about 0.03, which were evaluated with Equation (3.1), at each flow node (or at each station) as given in Table 3.2. Since JAEA has not provided PNNL with the shapes of the river cross-sections, a rectangular shape was used for the flow cross-section evaluation by CHARIMA; specifically, the flow area is the flow width times the flow depth. The velocities in Table 3.2 were evaluated by dividing the flow rate by the flow area.

The data listed in Table 3.2 are plotted in Figure 3.1 through Figure 3.3. Figure 3.1 presents the variations of the elevation (thalweg) and the width of the Ukedo River used for the TODAM modeling.

Table 3.2. Geometry and Flow Parameters Evaluated by CHARIMA for Ukedo River Modeling by TODAM.

Node	Station (km)	Flow (m^3/s)	Velocity (m/s)	Area (m^2)	Thalweg (m)	Width (m)	Depth (m)	Manning Roughness, n
1	22	4.19	1.42	2.96	102.00	10.0	0.30	0.033
2	21	4.19	1.42	2.96	90.00	10.0	0.30	0.033
3	20	4.88	1.50	3.24	78.00	10.0	0.32	0.033
4	19	4.88	1.50	3.24	66.00	10.0	0.32	0.033
5	18	5.58	1.60	3.49	54.00	10.0	0.35	0.032
6	17	5.58	1.26	4.44	42.00	20.0	0.22	0.032
7	16	6.28	0.82	7.68	30.00	20.0	0.38	0.032
8	15	6.28	0.58	10.91	27.50	50.0	0.22	0.031
9	14	6.28	0.58	10.92	25.00	50.0	0.22	0.031
10	13	6.28	0.56	11.18	22.50	50.0	0.22	0.033
11	12	6.28	0.80	7.86	20.00	20.0	0.39	0.033
12	11	6.28	0.80	7.86	17.50	20.0	0.39	0.033
13	10	6.28	0.80	7.86	15.00	20.0	0.39	0.033
14	9	6.28	0.80	7.86	12.50	20.0	0.39	0.033
15	8	6.28	0.80	7.86	10.00	20.0	0.39	0.033
16	7	6.28	0.78	8.00	7.50	20.0	0.40	0.034
17	6	6.28	0.57	11.06	5.00	20.0	0.55	0.033
18	5	6.28	0.57	11.01	4.17	20.0	0.55	0.033
19	4	6.28	0.58	10.92	3.33	20.0	0.55	0.032
20	3	6.28	0.62	10.13	2.50	20.0	0.51	0.029
21	2	6.28	0.32	19.49	1.67	80.0	0.24	0.035
22	1	12.56	0.40	31.73	0.83	80.0	0.40	0.039
23	0	12.56	0.66	18.90	0.00	30.0	0.63	0.031

A comparison with Figure 1.2 shows that Figure 3.1 is adequate for the TODAM modeling for the region from the location below the Ougaki Dam to the river mouth at the Pacific Ocean.

Figure 3.2 presents the flow rates and velocities used for TODAM modeling. The variations in area and depth of the Ukedo River used for the TODAM modeling are given in Figure 3.3. In Figure 3.2, it is seen that the velocity decreases, while the flow rate remains constant, in the region between 13 and 15 km from the river mouth. Using Figure 3.1 and Figure 3.3, this velocity decrease is explained by the increase in the flow area due to the increase in the flow width, though the flow depth decreases, in this region.

Figure 3.2 shows that the velocity decreases, while the flow rate and flow width remain constant, in the region between 3 and 6 km from the river mouth. Using Figure 3.1 and Figure 3.3, this velocity decrease is explained by the increase in the flow area by the increase in the flow depth due to the smaller river slope in this region.

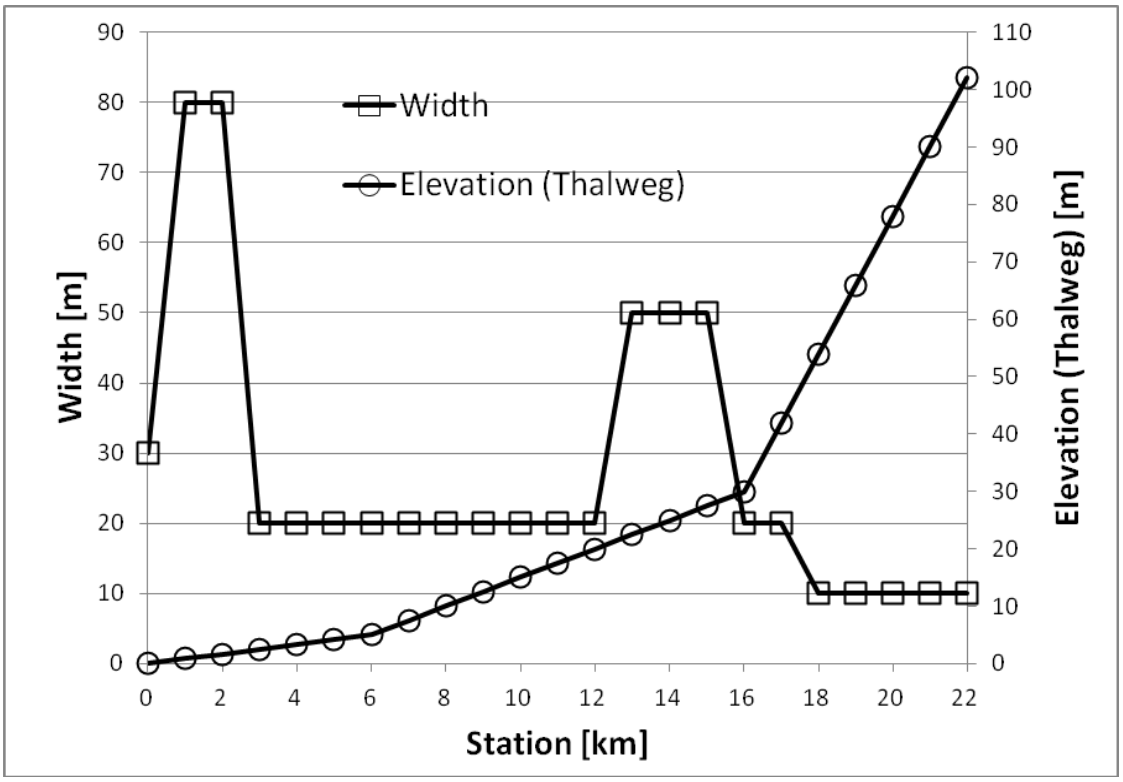

Figure 3.1. Variations of Elevation (thalweg) and Width of the Ukedo River Used for TODAM Modeling

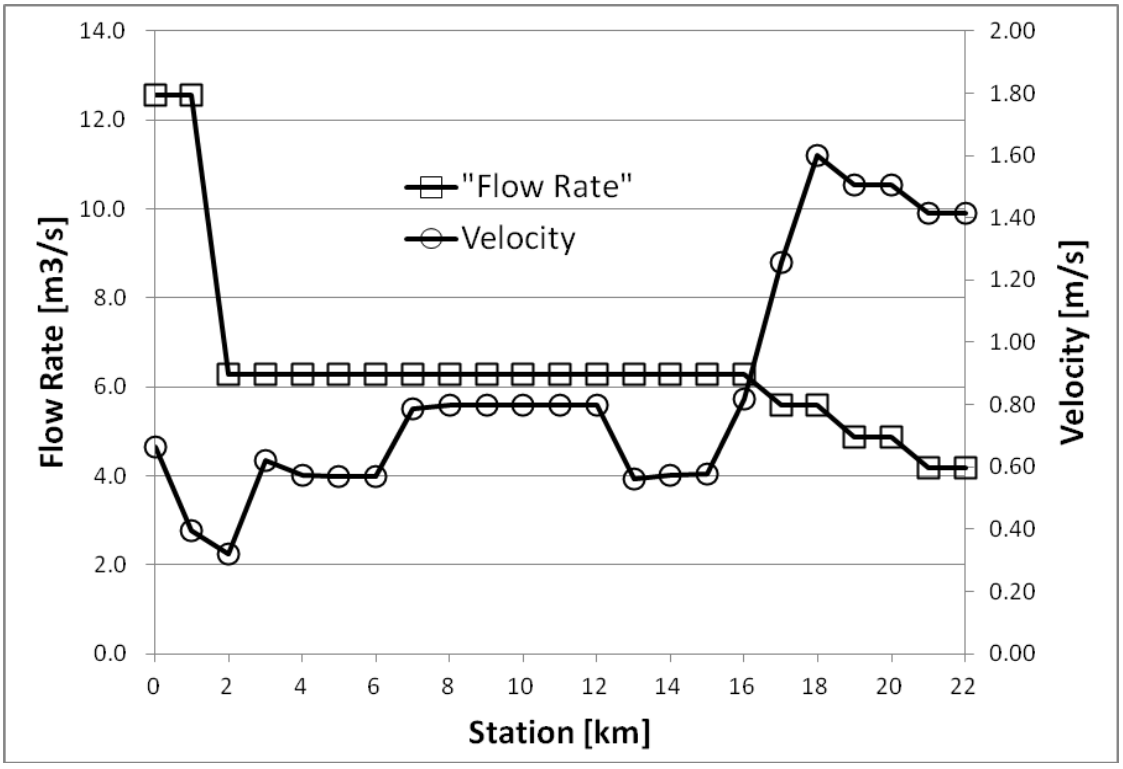

Figure 3.2. Flow Rate and Velocity of the Ukedo River Used for TODAM Modeling.

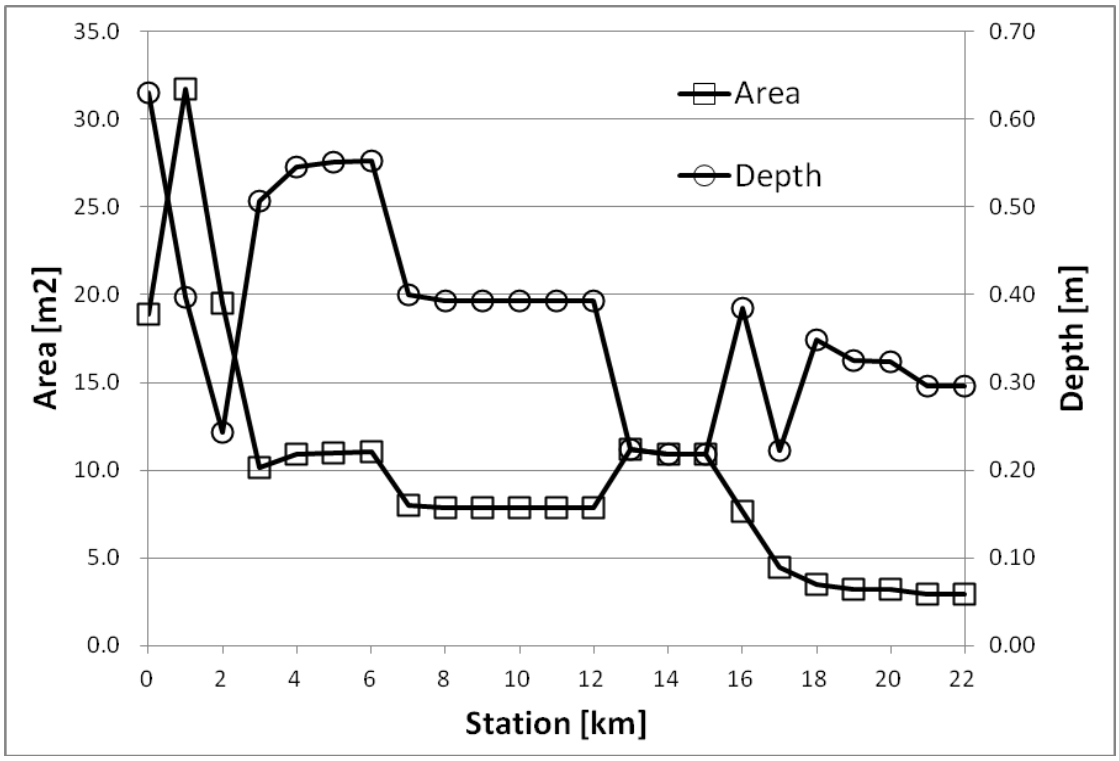

Figure 3.3. Variations of Area and Depth of the Ukedo River Used for TODAM Modeling

A large velocity decrease is seen in Figure 3.2 in the region between 1 and 2 km from the river mouth. This region is significantly influenced by the confluence of the Ukedo and the Takase rivers. As seen in Figure 3.1 and Figure 3.3, this velocity decrease is explained by the increase in the flow area probably due to the confluence of the Ukedo and the Takase rivers.

Finally, at the river mouth, the flow depth significantly increases because of the decrease in the flow width at this point, while the flow rate remains as high as 12.56 m^3/s due to the confluence of the Ukedo and the Takase rivers.

The data given in Table 3.2 with their plots of Figure 3.1, Figure 3.2, and Figure 3.3 provide the basis for the analysis of TODAM Ukedo River modeling in the later subsection.

3.2.1 Grid and Input Data

As described in detail in the previous section, the TODAM modeling of the Ukedo River was conducted with the flow data produced by CHARIMA. In addition to the flow data produced by CHARIMA, this subsection outlines all of the input data files used for the TODAM Ukedo River Simulation.

Brief descriptions of the input data files are as follows:[1]

- Configuration file (todam.input) to provide the general information by specifying the input files or the data to be used for the simulation;

[1] The name in the parentheses is the file name used for the TODAM simulation.

- Problem layout file (segment.data) to provide the definitions of segments and junctions with the nodes which are used for the computations by TODAM;
- Geometry file (geometry.data) to provide the physical dimensions of the model at each node;
- Hydrodynamics file (hydrology.data) to provide the hydrodynamics data for the simulation;
- Initial bed conditions file (initial_bed.data) to provide the initial bed depth, sediment size fraction, and contaminant concentration;
- Initial water column conditions file (initial_conc.data) to provide the initial water column concentration of the sediment and contaminant;
- Upstream boundary conditions file (boundary.data) to provide the concentration of the sediment and contaminant at the upstream boundary nodes;
- Dispersion coefficients file (dispersion.data) to provide the longitudinal dispersion coefficients used for the computation domain;
- Critical bed stresses file (critical_stresses.data) to provide the critical erosion and deposition stresses for the cohesive sediments, silt and clay;
- Erosion coefficients file (erosion.data) to provide the armoring and erodibility coefficients;
- Contaminant sorption properties file (contaminant.data) to provide the contaminant distribution coefficients and the mass transfer rates for the contaminant between the dissolved, suspended, and bed sediments; and
- Tributary contributions file (tributary.data) to provide the sediment concentrations or loads and the contaminant concentrations or loads from lateral inflow or tributaries.

The geometry file (geometry.data) and the hydrodynamics file (hydrology.data) were produced by CHARIMA as described in the previous section.
The following were specified for the conducted TODAM simulation of Ukedo River:

- A unsteady transport simulation with ^{137}Cs contaminant for 100 hours;
- Fluid stresses were computed internally by TODAM;
- The Toffaleti formula was used to compute the sediment transport capacity;
- Constant hydrodynamics data were used for the 100-hour simulation;
- Initial bed layer thickness of 0.27 m was assigned;
- 40% of the sand mass fraction, 40% of the silt mass fraction, and 20% of the clay mass fraction were assigned in the initial bed layer;
- No ^{137}Cs contaminant was included in the initial bed layer;
- No sediment fractions and ^{137}Cs contaminant were included in the initial water flow;
- Dissolved ^{137}Cs contaminant concentration of 1000 Bq/m^3 was introduced at the upstream boundary of 22 km from the river mouth;

- Sediment concentrations and ^{137}Cs contaminant concentrations from lateral inflow or tributaries were not applied; and
- Dispersion coefficients evaluated by using Equation (3.2) were used.

$$\varepsilon_x = \frac{UB^2}{3D} \tag{3.2}$$

where ε_x = longitudinal dispersion coefficients,
U = flow velocity,
B = flow width, and
D = flow depth.

In Equation (3.2), for $\varepsilon_x > 500$, $\varepsilon_x = 500$ was used.

3.2.2 Preliminary Model Results

A TODAM simulation of the Ukedo River was conducted with the input data described in the previous subsection. TODAM simulated

- within the water column, distributions of concentrations of
    - suspended sand,
    - suspended silt
    - suspended clay
    - dissolved ^{137}Cs
    - particulate ^{137}Cs sorbed by suspended sand
    - particulate ^{137}Cs sorbed by suspended silt, and
    - particulate ^{137}Cs sorbed by suspended clay
- within the river bottom, distributions of
    - river bed elevation changes due to suspended sediment deposition to the river bottom and/or erosion of the river bed
    - longitudinal and vertical distributions of sediment fractions of river bottom sand, river bottom silt and river bottom clay
    - ^{137}Cs concentrations sorbed by river bottom sand
    - ^{137}Cs concentrations sorbed by river bottom silt

- ^{137}Cs concentrations sorbed by river bottom clay.

This subsection presents the results of the TODAM simulation at a 100-hour run.

Figure 3.4 presents the suspended sediment concentrations of sand, silt, and clay at the 100-hour TODAM simulation time. As the initial condition, no sediment fractions were included in the water flow. Therefore, the sediments of sand, silt, and clay seen in Figure 3.4 were eroded from the bed layer and suspended in the flow. As expected, sand was eroded from the bed more than silt and clay were. Silt was eroded from the bed more than clay was because the critical bed shear stress for erosion for silt is lower than that for clay and the critical bed shear stress for deposition for silt is higher than that for clay. Along with the flow in the downstream direction, both the processes of sediment suspension and deposition are expected to occur.

From Figure 3.4, the significant suspension is seen for sand in the region between 16 and 18 km from the river mouth. This is considered to be because the flow velocity is higher in the upstream until it gets to the point of 17 km from the river mouth (see Figure 3.2). The less suspension of sand is seen in the upstream region beyond 18 km from the river mouth. This is considered to be because sand of the bed layer in the upstream region was almost completely eroded and was transported downstream at the 100-hour simulation time.

It is seen from Figure 3.4 that the suspension of sand decreased in the downstream direction from the location of 15 km from the river mouth. The flow velocity drastically decreased at this point (see Figure 3.2). Therefore, the flow momentum is significantly reduced and consequently the quantity of sand suspension was reduced at this location. As a matter of fact, the largest deposition occurred, in this simulation, at the locations between 15 and 16 km from the river mouth, as discussed in the following (shown in Figure 3.5).

A fair amount of sand suspension is seen in the region from the location of 17 to 15 km in Figure 3.4. It is considered that the quantity of sand eroded and suspended in the upstream region and transported downstream was so large and a fair amount of sand was still suspended though a large amount of sand was deposited in the region between 15 and 16 km from the river mouth.

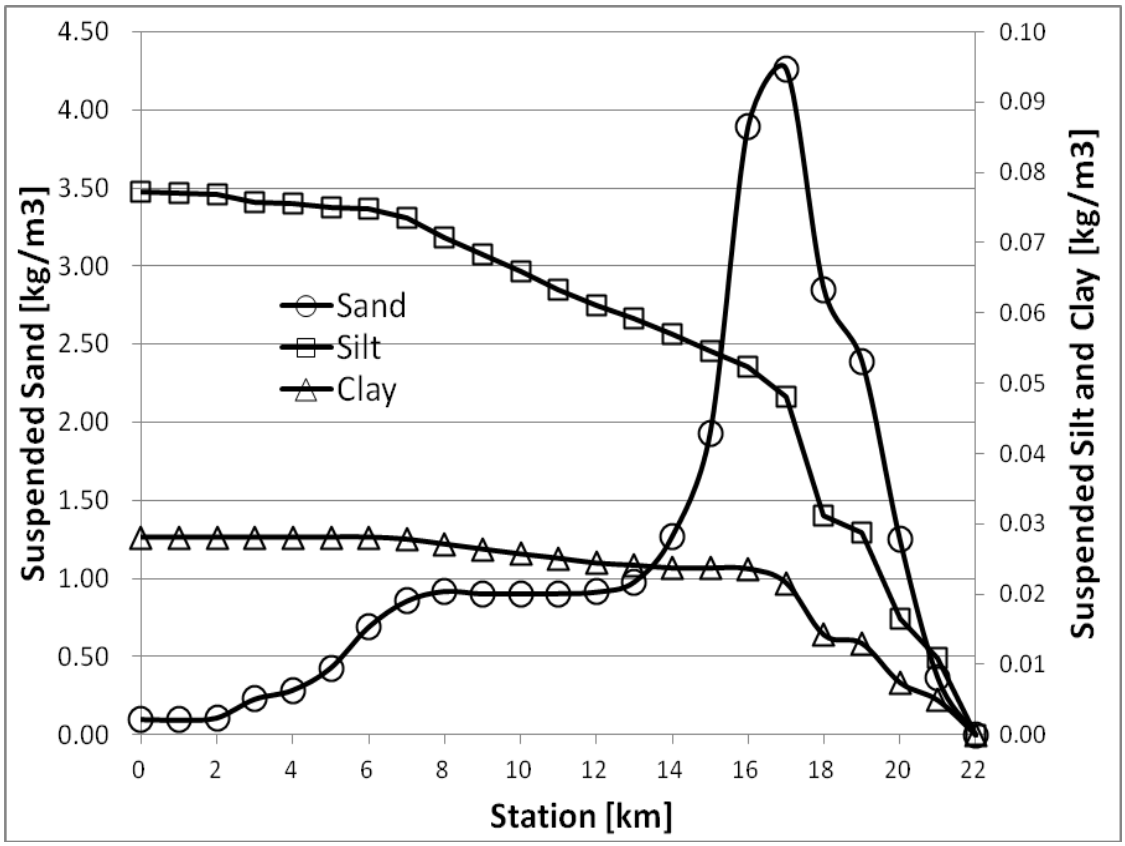

Figure 3.4. Computed Suspended Sediment Fractions at 100-hour TODAM Simulation Time.

As seen in Figure 3.2, the flow velocity increased between 7 and 12 km from the river mouth and Figure 3.4 shows that the suspended sand concentrations remained constant, which indicates no significant sand deposition occurred, in this region. From 3 to 6 km, the flow velocity decreased that resulted in a reduction in the sand suspension in this region as seen in Figure 3.4. The flow velocity further decreased at 2 km from the river mouth but the suspended sand concentration remained constant from 2 km to the river mouth. This is considered to be because the flow depth increased in this region, as seen in Figure 3.3, and the increased depth reduced the sand deposition as the settling distance was increased.

Generally, the suspension of both silt and clay increased along with the flow in the downstream direction as seen in Figure 3.4. This is expected because silt and clay are not as erodible as sand is and the quantity of silt and clay eroded from the bed layer in the upstream flow was small and the suspended silt and clay were not significantly deposited along the flow in the downstream direction.

Figure 3.5 shows the computed bed layer thickness developed at the 100-hour TODAM simulation time. The bed layer thickness shown in Figure 3.5 includes all of sediment fractions of sand, silt, and clay. Figure 3.5 shows the thickness is less than the initial bed layer thickness from the upstream boundary to the point of 16 km from the river mouth. This indicates the erosion process dominated in this upstream region.

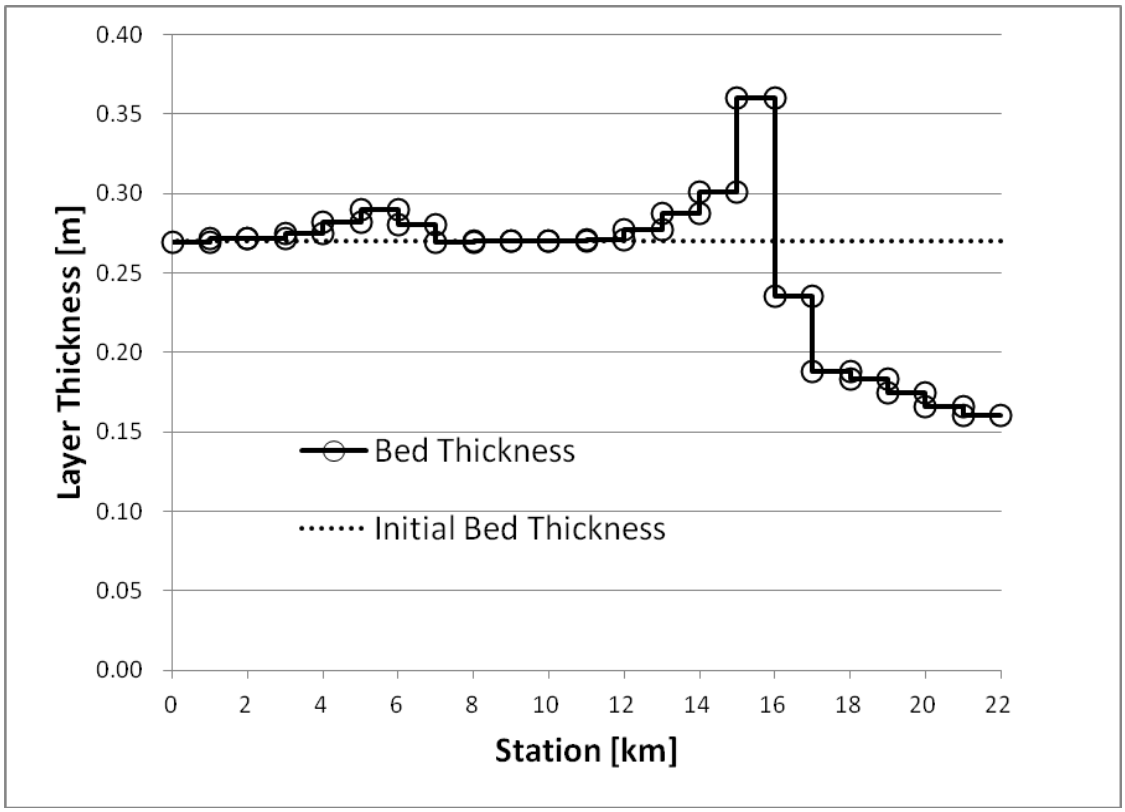

Figure 3.5. Computed Bed Layer Thickness at 100-hour TODAM Simulation Time.

As discussed above, it is considered that most of the suspended sand was eroded from the bed layer from the upstream boundary to the point of 17 km from the river mouth. Therefore, the remained bed layer consisted mostly of silt and clay in this region. Also, as discussed above, it is considered that the thickness of the bed layer between 15 and 16 km, seen in Figure 3.5, increased mostly due to the deposition of sand.

Figure 3.4 shows that the slopes of the suspension rate of silt and clay decreased at the location of 16 km from the river mouth. This indicates that the deposition of silt and clay occurred at this point. However, the quantity of the deposited silt and clay is considered to be small compared with that of sand because the suspended silt and clay remained to increase while the suspended sand decreased.

Another increase in the bed layer thickness is seen in the region between 4 and 7 km from the river mouth in Figure 3.5. Figure 3.4 shows, at the point of 7 km from the river mouth, a decrease in the slopes of the suspension rate of silt and clay and a significant decrease in the suspension of sand. From Figure 3.2, the flow velocity decreased at 6 km from the river mouth. It is considered that the decrease in the flow momentum by the decrease in the flow velocity caused the increase in the deposition in this region.

The flow velocity further decreased at 2 km from the river mouth but the suspended silt and clay remained constant. This is considered to be because the flow depth increased in this region, as seen in Figure 3.3, and the increased depth reduced the silt and clay deposition in the same manner as the case of sand.

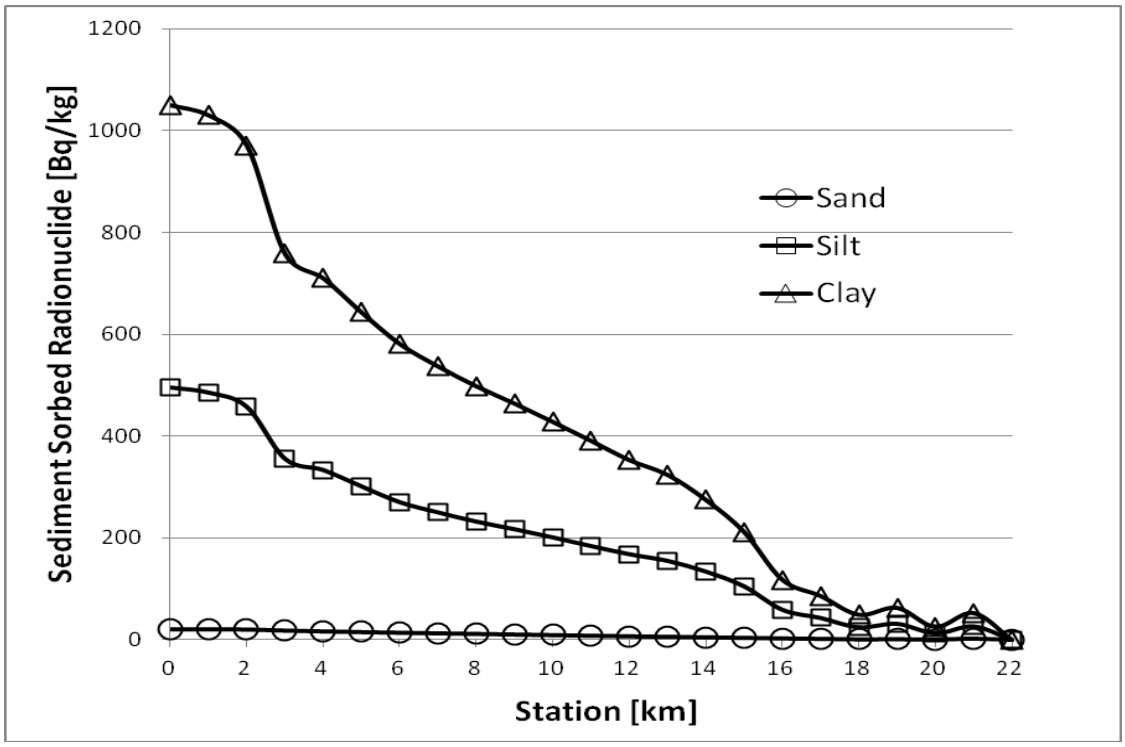

Figure 3.6. Computed Sediment-Sorbed ^{137}Cs Radionuclide (contaminant) in Flow at 100-Hour TODAM Simulation Time.

Figure 3.6 shows the concentrations of ^{137}Cs adsorbed by the suspended sediments of sand, silt, and clay in the flow at the 100-hour TODAM simulation time.

Since no sediment fractions and radionuclide (contaminant) were included in the initial water flow, the source of cesium seen in Figure 3.6 was the dissolved cesium concentration of 1000 Bq/m^3 introduced at the upstream boundary of 22 km from the river mouth, as described in the previous subsection, as the boundary condition.

The quantity of cesium adsorbed by clay was greatest and sand adsorbed the smallest quantity of cesium. This is because the distribution coefficient between the dissolved cesium and the clay-sorbed cesium is greatest and the distribution coefficient between the dissolved cesium and the sand-sorbed cesium is smallest.

It is seen from Figure 3.6 that the cesium continues to be adsorbed by the sediments as it flows from the upstream boundary to the river mouth. The absorption rate was small until the flow gets to the point of 16 km from the river mouth. This is considered to be because that the suspension of silt and clay is still small in this region as seen in Figure 3.4.

Figure 3.4 shows that the suspension of silt and clay increased from the point of 17 km to the downstream direction. This increase in the silt and clay suspension is considered to result in the proportional increase in the cesium adsorbed by the silt and clay in this region, as seen in Figure 3.6.

A drastic increase in the cesium adsorbed by the silt and clay at 2 km from the river mouth is seen in Figure 3.6. This is considered to be because the flow velocity decreased significantly at this point, as seen in Figure 3.2, which extended the adsorption time.

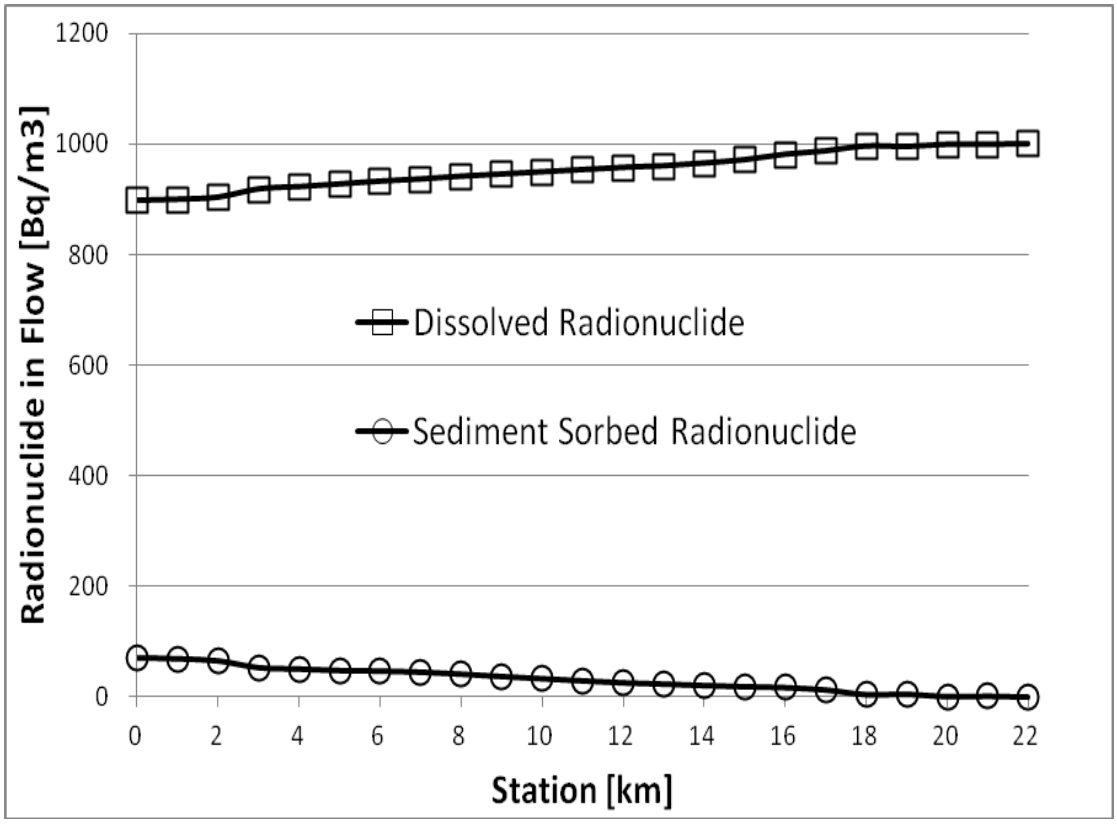

Figure 3.7. Computed Total ^{137}Cs (contaminant) in the Flow at 100-Hour TODAM Simulation Time.

Figure 3.7 shows the total ^{137}Cs radionuclide (contaminant) in the flow at 100-hour TODAM simulation time. Initially, the water flow did not include sediment fractions and cesium radionuclide. Then, the dissolved cesium concentration of 1000 Bq/m^3 was introduced at the upstream boundary of 22 km from the river mouth as the boundary condition.

As the TODAM simulation advanced in time, this cesium concentration introduced at the upstream boundary continued to be transported and dispersed in the downstream flow direction and, in the flow, some cesium was adsorbed by the sediments of sand, silt, and clay, as discussed above.

The total of cesium adsorbed by sand, silt, and clay is given as the sediment-sorbed radionuclide in Figure 3.7. The dissolved radionuclide given in Figure 3.7 is the remains of cesium in the flow. Essentially Figure 3.6 is equivalent to the sediment-sorbed radionuclide in Figure 3.7.

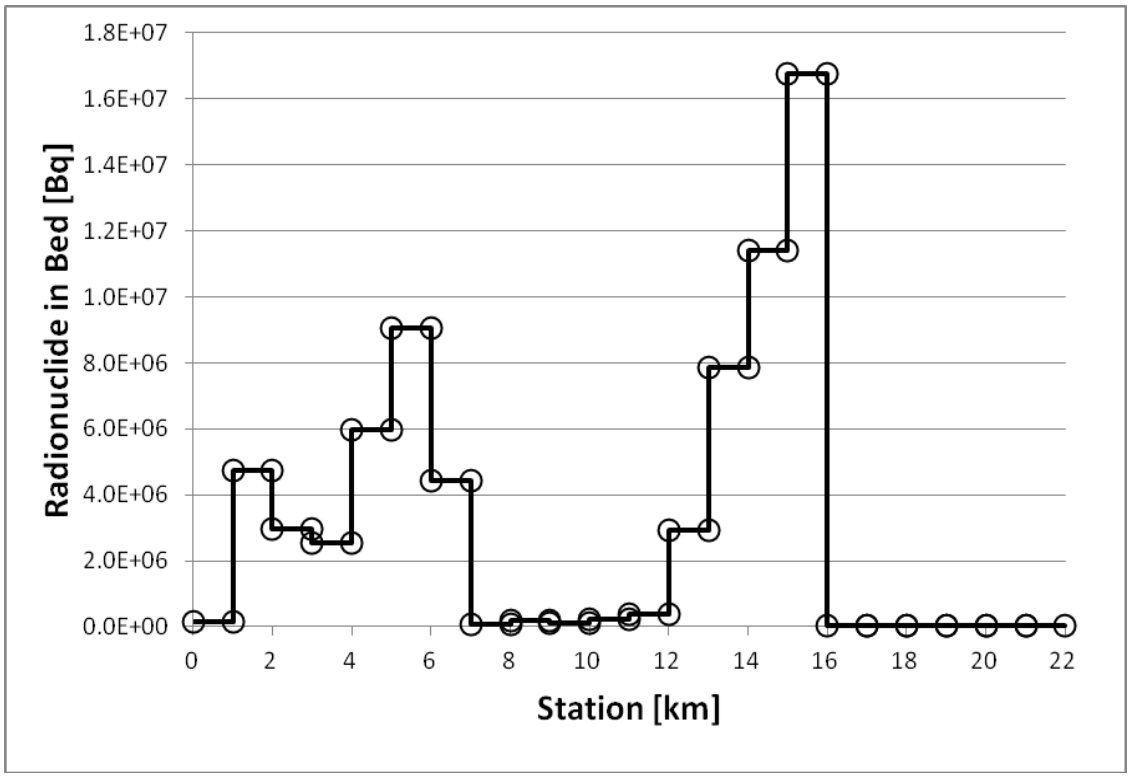

Figure 3.8. Computed Total ^{137}Cs (contaminant) in the Bed Layer at 100-Hour TODAM Simulation Time.

Figure 3.8 shows the total ^{137}Cs (contaminant) deposited in the bed at 100-hour TODAM simulation time. As described in the previous subsection, cesium was not initially included in the bed layer. The dissolved cesium concentration of 1000 Bq/m^3 introduced at the upstream boundary was transported and dispersed in the downstream flow direction.

In the flow, some of the dissolved cesium was adsorbed by the suspended sediments of sand, silt, and clay, and some of the suspended sand, silt, and clay which adsorbed cesium were deposited on the river bottom. In addition to the deposition of cesium adsorbed by the suspended sand, silt, and clay, some of the cesium was deposited on the bed by the adsorption directly from the dissolved cesium in the flow. Figure 3.8 shows the total of the cesium in the bed layer.

By the comparison of Figure 3.8 with Figure 3.5, it is seen that the most cesium in the bed layer was deposited through the sediment deposition process except the region between 1 and 2 km from the river mouth. As seen in Figure 3.2, the significant decrease in the velocity in the region between 1 and 2 km is considered to result in the increase in the cesium deposition by the adsorption directly from the dissolved cesium in the flow.

Figure 3.9. Computed Total ^{137}Cs (contaminant) in the 7th Segment Bed Layer at 100-Hour TODAM Simulation Time.

Figure 3.9 shows the total ^{137}Cs (contaminant) in the 7th segment bed layer, the region between 15 and 16 km from the river mouth, at 100-hour TODAM simulation time. In Figure 3.9, the position of 0 (zero) m indicates the top of the bed layer and the cesium is deposited in the manner shown in Figure 3.9 in the TODAM simulation.

4.0 Summary

The Fukushima Daiichi Nuclear Power Plant nuclear accident released ^{131}I, ^{134}Cs and ^{137}Cs to the environment, in addition to very small amounts of ^{89}Sr, ^{90}Sr, ^{238}Pu, and $^{239\text{-}240}Pu$. Some portions of ^{134}Cs and ^{137}Cs deposited on land surface were adsorbed by the surface soil and will be washed off from the ground surface to receiving rivers by runoff water and snowmelt. Then, it is expected that the rivers will transport ^{134}Cs and ^{137}Cs downstream to the Pacific Ocean while depositing some of which on the river bottom.

To simulate the cesium migration and accumulation in the rivers, the time-varying, one-dimensional sediment-contaminant transport code TODAM was applied to a unsteady, one-dimensional model of the Ukedo River in Fukushima from the location below the Ougaki Dam to the river mouth at the Pacific Ocean. This TODAM simulation evaluates the amount and locations of cesium accumulation in rivers and radionuclide discharges of dissolved and sediment-sorbed cesium flowing into the Pacific Ocean.

A TODAM simulation was conducted for a preliminary Ukedo River model herein. The conducted TODAM simulation of the preliminary Ukedo River modeling is summarized as follows:

1. JAEA provided the flow rates, river bottom elevations, and flow widths for the Ukedo River modeling by TODAM;
2. Based on the data given in 1), CHARIMA evaluated the flow areas, velocities, and depths with a rectangular cross-section of the area;
3. For the CHARIMA run of 2), Manning numbers of 0.03 to 0.04 were used;
4. The TODAM Ukedo River modeling was conducted as:

- A unsteady transport simulation with ^{137}Cs contaminant for 100 hours;
- Fluid stresses were computed internally by TODAM;
- Sediment was divided into sand, silt and clay fractions;
- The Toffaleti formula was used to compute the sand transport capacity;
- Constant hydrodynamics data were used for the 100-hour simulation;
- Initial bed layer thickness of 0.27 m was assigned;
- 40% of the sand mass fraction, 40% of the silt mass fraction, and 20% of the clay mass fraction were assigned in the initial bed layer;
- No ^{137}Cs contaminant was included in the initial bed layer;
- No suspended sediments and ^{137}Cs contaminant were included in the initial water flow;
- Both dissolved and particulate ^{137}Cs sorbed by both suspended and river bottom sediments of sand, silt and clay were simulated in the water column and within the river bottom;
- Dissolved ^{137}Cs contaminant concentration of 1000 Bq/m^3 was introduced at the upstream boundary of 22 km from the river mouth;

- Sediment concentrations and ^{137}Cs contaminant concentrations from lateral inflows or tributaries were not applied; and
- Dispersion coefficients were evaluated by using Equation (3.2), $\varepsilon_x = \frac{UB^2}{3D}$;

5. The results of the TODAM simulation at a 100-hour run include:

- Along with the flow in the downstream direction, both the processes of sediment suspension and deposition occurred.
- River bed erosion process dominated in the region from the upstream boundary to the point of 16 km from the river mouth.
- The largest sediment deposition occurred in the region between 15 and 16 km from the river mouth.
- The second sediment deposition occurred in the region between 4 and 7 km from the river mouth.
- Sand was eroded from the bed more than silt and clay were, and silt was eroded from the bed more than clay was.
- Significant suspension occurred for sand in the region between 16 and 18 km from the river mouth.
- The suspension of sand significantly decreased at the locations between 15 and 16 km from the river mouth where the largest deposition occurred in the simulation.
- The suspended sand concentrations remained constant in the region between 7 and 12 km from the river mouth.
- The sand suspension decreased from 3 to 6 km but the suspended sand concentration remained constant from 2 km upstream of the river mouth to the river mouth.
- Generally, the suspended concentrations of both silt and clay increased along with the flow in the downstream direction.
- The suspension rates of silt and clay decreased first at the location 16 km from the river mouth and further decreased at 7 km above the river mouth.
- Most of the dissolved cesium introduced at Ougaki Dam (22 km from the river mouth) was continuously transported and dispersed in the downstream flow direction.
- In the flow, some of the dissolved cesium was adsorbed by the suspended sand, silt, and clay, and some of the suspended sand, silt, and clay which adsorbed cesium were deposited on the river bottom.
- In addition to the deposition of cesium adsorbed by the suspended sand, silt, and clay, some of the dissolved cesium was directly adsorbed by the bottom sediment, further contaminating the river bed
- The quantity of cesium adsorbed by the suspended clay was greatest and the suspended sand adsorbed the smallest quantity of cesium.
- The cesium absorption by the suspended silt and clay first increased at the point 16 km from the river mouth and a further increase in the cesium absorption by the suspended silt and clay occurred at 2 km, where the Takase River merges with the Ukedo River .

- The most cesium in the river bed layer was deposited through the sediment deposition process except in the region between 1 and 2 km from the river mouth.

The preliminary Ukedo River modeling conduced here provides a basis for a future detailed analysis of TODAM Ukedo River modeling.

5.0 References

Chow VT. 1959. *Open Channel Hydraulics.* McGraw-Hill Book Company, New York, New York.

Colby BR. 1964. "Discharge of Sands and Mean Velocity Relationships in Sand-Bed Streams." Geological Survey Professional Paper 462-A, U.S. Geological Survey, Washington, D.C.

Du Boys P. 1879. "Le Rohne et les Riveieres a Lit Affouillable." *Annales des Ponts et Chaussees,* Series 5, Vol. 18, pp. 141-195.

FM Holly Jr., JC Yang, P Schwarz, J Schaefer, SH Hsu and R. Einhellig. 1990. *Numerical Simulation of Unsteady Water and Sediment Movement in Multiply Connected Networks of Mobile-Bed Channels*. IIHR Report No. 343. Iowa Institute of Hydraulic Research. The University of Iowa. Iowa City, Iowa, 52242 USA.

Graf WH. 1971. *Hydraulics of Sediment Transport.* McGraw-Hill Book Co., New York, New York.

Krone RB. 1962. *Flume Studies of the Transport of Sediment in Estuarial Shoaling Processes*. Hydraulic Engineering and Sanitary Engineering Research Laboratory, University of California, Berkeley.

MEXT – Ministry of Education, Culture, Sport, Science and Technology of Japan. 2011. *http://radioactivity.mext.go.jp/ja/*.

Onishi Y, OV Voitsehkovich and MJ Zheleznyak, Eds. 2007. *Chernobyl – What Have We learned? The Successes and Failures to Mitigate Water Contamination Over 20 years.* Springer Publishers, Dordrecht, The Netherlands.

Partheniades E. 1962. *A Study of Erosion and Deposition of Cohesive Soils in Salt Water*. Ph.D. Thesis, University of California, Berkeley, California.

Toffaleti FB. 1969. "Definitive Computations of Sand Discharge in Rivers." *Journal of Hydraulic Division,* American Society of Civil Engineers, Vol. 95, No. HYI. Proc. Paper 6350, pp. 225–248.

Vanoni VP, Ed. 1975. *Sedimentation Engineering*. ASCE Manuals and Report on Engineering Practice, American Society of Civil Engineers, New York, New York.

Pacific Northwest
NATIONAL LABORATORY

Proudly Operated by **Battelle** *Since 1965*

U.S. DEPARTMENT OF
ENERGY

902 Battelle Boulevard
P.O. Box 999
Richland, WA 99352
1-888-375-PNNL (7665)
www.pnnl.gov